

Thermodynamic Geometry of Microscopic Heat Engines

Kay Brandner¹ and Keiji Saito²

¹*Department of Applied Physics, Aalto University, 00076 Aalto, Finland and*

²*Department of Physics, Keio University, 3-14-1 Hiyoshi, Yokohama 223-8522, Japan*

We develop a geometric framework to describe the thermodynamics of microscopic heat engines driven by slow periodic temperature variations and modulations of a mechanical control parameter. Covering both the classical and the quantum regime, our approach reveals a universal trade-off relation between efficiency and power that follows solely from geometric arguments and holds for any thermodynamically consistent microdynamics. Focusing on Lindblad dynamics, we derive a second bound showing that coherence as a genuine quantum effect inevitably reduces the performance of slow engine cycles regardless of the driving amplitudes. To demonstrate the practical applicability of our results, we work out the example of a single-qubit heat engine, which lies within the range of current solid-state technologies.

The laws of thermodynamics put fundamental limits on the performance of thermal machines across all length and energy scales. A prime example is the Carnot bound on efficiency, which applies to James Watt's steam engine as well as to recent small-scale engines using colloidal particles [1–3], single atoms [4, 5] or engineered quantum systems [6, 7]. Still, despite its universality, this bound is mostly of theoretical value as it can be attained only by infinitely slow cycles producing zero power. Practical devices, however, must operate in finite time and therefore are inevitably subject to frictional energy losses suppressing their efficiency. Hence, we are prompted to ask: how much performance has to be sacrificed for finite speed?

This question, which inspired the development of finite-time thermodynamics in the 1970s [8], has recently attracted renewed interest: triggered by the observation that Carnot efficiency at finite power could indeed be possible in systems with broken time-reversal symmetry [9], a series of studies discovered quantitative trade-off relations, which limit the finite-time performance of microscopic engines and confirm the conventional expectation that dissipationless machines deliver zero power [10–17].

These results rely on stochastic models to describe the internal dynamics of small-scale engines. Here, we pursue an alternative strategy that builds on the framework of thermodynamic geometry [18]. This approach replaces the traditional thermodynamic picture, which mixes control and response variables, with a geometric picture. The properties of the working system are thereby encoded in a vector potential and a Riemannian metric in the space of control parameters, see Fig. 1. The driving protocols define a closed path in this space and can thus be assigned an effective flux and length. In adiabatic response, these quantities provide measures for the two key figures of merit: the work output and the minimal dissipation of the underlying thermodynamic process.

The idea of using geometric concepts to describe the thermodynamics of finite-time operations was originally conceived for macroscopic systems and developed mainly on the basis of phenomenological principles [8, 18, 19]. Over the last decades, this approach has been formu-

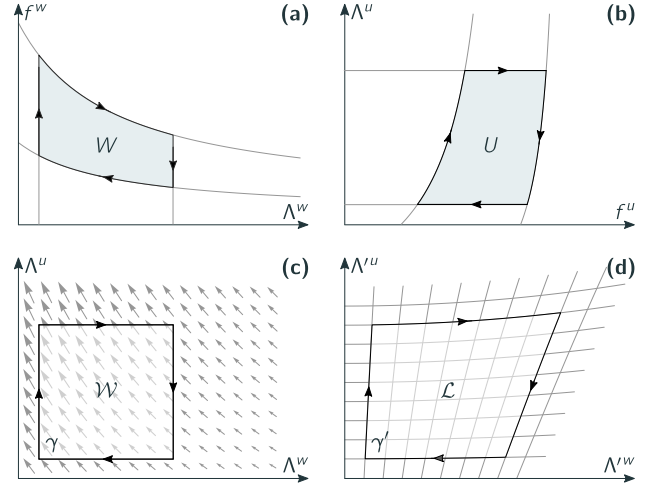


FIG. 1. Four faces of a microscopic engine cycle. Upper panel: Thermodynamic picture. The two sketches show effective pressure-volume (a) and temperature-entropy (b) diagrams for a Stirling cycle consisting of two *isochoric* ($\Lambda^w = \text{const}$) and two *isothermal* ($\Lambda^u = \text{const}$) strokes. The enclosed areas correspond to the generated work W and the effective thermal energy uptake U . Lower panel: Geometric picture. In the space of control parameters Λ^u and Λ^w , the adiabatic work W is given by the line integral of the thermodynamic vector potential along γ , i.e., the flux of the corresponding effective magnetic field through the area encircled by this path (c). In the curvilinear coordinates Λ'^w and Λ'^u , which carry the thermodynamic metric, γ is distorted into the contour γ' , whose length L provides a lower bound on the dissipated energy (d).

lated on microscopic grounds [20], linked to information-theoretic quantities [18] and extended to classical nanoscale systems [21], closed quantum systems far from equilibrium [22] and, most recently, open quantum systems [23]. Thermodynamic geometry has thus become a powerful tool, which, as its key application, provides an elegant way to determine optimal control protocols minimizing the dissipation of isothermal processes [23–27]. Yet, this framework has neither been applied systematically to bound the performance of cyclic micro-engines nor to explore the impact of quantum effects on such devices.

To progress in this direction, we consider a general model for a microscopic heat engine consisting of two components: a working medium with tunable Hamiltonian H_λ and a heat source to control the temperature T of the environment of this system. The device is operated by periodically changing the parameters λ and T such that the vector

$$\mathbf{\Lambda} \equiv (T, \lambda) \equiv (\Lambda^u, \Lambda^w) \quad (1)$$

passes through a closed path $\gamma: t \mapsto \mathbf{\Lambda}_t$. Once the system has settled to a periodic state ρ_t , the average output and input of this process, i.e., the mean generated work and the effective uptake of thermal energy from the heat source, are given by

$$W = \int_0^\tau dt f_t^w \dot{\Lambda}_t^w \quad \text{and} \quad U = - \int_0^\tau dt f_t^u \dot{\Lambda}_t^u. \quad (2)$$

Here, dots indicate time derivatives, τ denotes the cycle time and the thermodynamic forces,

$$f_t^w \equiv -\text{Tr}[\rho_t \partial_\lambda H_\lambda] \big|_{\lambda=\lambda_t} \quad \text{and} \quad f_t^u \equiv -\text{Tr}[\rho_t \ln \rho_t], \quad (3)$$

correspond to the generalized pressure and the entropy of the working system, respectively. The upper panel of Fig. 1 shows a graphical illustration of this scheme. Note that we set Boltzmann's constant to 1 throughout.

Using the relations (2), the energy balance of the engine can be formulated as

$$A \equiv U - W = - \int_0^\tau dt f_t^\mu \dot{\Lambda}_t^\mu \geq 0, \quad (4)$$

where $\mu = w, u$ and summation over identical indices is understood throughout. The quantity A corresponds to the mean energy loss or *dissipated availability* [28] per cycle; it must be non-negative as a direct consequence of the second law [29]. Thus, the dimensionless coefficient

$$\eta \equiv W/U \leq 1 \quad (5)$$

provides a proper measure for the efficiency of the engine. This figure is well-defined for any control protocols leading to positive work extraction, i.e., $W > 0$. In the special case, where the temperature switches between two constant levels, it becomes an upper bound on the traditional thermodynamic efficiency, which involves only the heat uptake during the hot phase of the cycle [30].

Under quasi-static driving, the system follows its instantaneous equilibrium state, i.e., we have

$$\rho_t = \varrho_{\mathbf{\Lambda}_t} \quad \text{with} \quad \varrho_{\mathbf{\Lambda}} \equiv \exp[-(H_\lambda - \mathcal{F}_{\mathbf{\Lambda}})/T] \quad (6)$$

and $\mathcal{F}_{\mathbf{\Lambda}}$ denoting the Helmholtz free energy. The generalized forces (3) can then be expressed as

$$f_t^\mu = \mathcal{F}_{\mathbf{\Lambda}_t}^\mu \quad \text{with} \quad \mathcal{F}_{\mathbf{\Lambda}}^\mu \equiv \text{Tr}[\varrho_{\mathbf{\Lambda}} F_{\mathbf{\Lambda}}^\mu] = -\partial_\mu \mathcal{F}_{\mathbf{\Lambda}}, \quad (7)$$

where we have introduced the force operators

$$F_{\mathbf{\Lambda}}^w \equiv -\partial_\lambda H_\lambda \quad \text{and} \quad F_{\mathbf{\Lambda}}^u \equiv -\ln \varrho_{\mathbf{\Lambda}} \quad (8)$$

for later purposes. Inserting (7) into (4) shows that the energy loss A goes to zero in the quasi-static limit; the efficiency (5) thus attains its upper bound 1. However, since the condition (6) can be met only for infinitely long cycle times, the generated power, $P \equiv W/\tau$, also vanishes and the engine becomes virtually useless.

Increasing the driving speed leads to finite power but inevitably also to energy losses reducing η . This trade-off can be understood quantitatively in the adiabatic response regime, where the external parameters change slowly compared to the relaxation time of the system. Under this condition, the thermodynamic forces (3) and the control rates $\dot{\mathbf{\Lambda}}_t$ are connected by the linear relations

$$f_t^\mu = \mathcal{F}_{\mathbf{\Lambda}_t}^\mu + R_{\mathbf{\Lambda}_t}^{\mu\nu} \dot{\Lambda}_t^\nu, \quad (9)$$

where $\nu = w, u$ and the adiabatic response coefficients $R_{\mathbf{\Lambda}_t}^{\mu\nu}$ depend parametrically on the driving protocols $\mathbf{\Lambda}_t$ [31]. The average energy loss (4) thus becomes

$$A = \int_0^\tau dt g_{\mathbf{\Lambda}_t}^{\mu\nu} \dot{\Lambda}_t^\mu \dot{\Lambda}_t^\nu \quad \text{with} \quad g_{\mathbf{\Lambda}}^{\mu\nu} \equiv -(R_{\mathbf{\Lambda}}^{\mu\nu} + R_{\mathbf{\Lambda}}^{\nu\mu})/2 \quad (10)$$

denoting the elements of a, possibly degenerate, metric tensor in the space of control parameters [32]. Thus, the Cauchy-Schwarz inequality implies

$$A \geq \mathcal{L}^2/\tau, \quad \text{where} \quad \mathcal{L} \equiv \oint_\gamma \sqrt{g_{\mathbf{\Lambda}}^{\mu\nu} d\Lambda^\mu d\Lambda^\nu} \quad (11)$$

corresponds to the thermodynamic length of the path γ .

Expanding the efficiency (5) to second order in the driving rates $\dot{\mathbf{\Lambda}}_t$ yields $\eta = 1 - A/\mathcal{W}$, where the adiabatic work can be expressed as a line integral,

$$\mathcal{W} = - \oint_\gamma \mathcal{A}_{\mathbf{\Lambda}}^\mu d\Lambda^\mu \quad \text{with} \quad \mathcal{A}_{\mathbf{\Lambda}}^\mu \equiv \partial_\mu \mathcal{F}_{\mathbf{\Lambda}}^w \Lambda^w \quad (12)$$

being the thermodynamic vector potential. Upon using (11), we thus arrive at our first main result, the power-efficiency trade-off relation

$$(1 - \eta)(\mathcal{W}/\mathcal{L})^2 \geq \mathcal{W}/\tau = P. \quad (13)$$

This bound implies that the power of any cyclic heat engine covered by our model must vanish at least linearly as its efficiency approaches the ideal value 1. The maximal slope of this decay is determined by the thermodynamic mean force \mathcal{W}/\mathcal{L} , where \mathcal{L} and \mathcal{W} are geometric quantities, i.e., they are independent of the parameterization of the control path γ , see the lower panel of Fig. 1.

Moreover, (13) entails a universal optimization principle, which arises from the observation that the bound (11) becomes an equality if the path γ is parameterized in terms of its thermodynamic length. To this end, t has to be replaced with the speed function ϕ_t , which is implicitly defined through the relation

$$t = \tau \int_0^{\phi_t} ds \sqrt{g_{\mathbf{\Lambda}_s}^{\mu\nu} \dot{\Lambda}_s^\mu \dot{\Lambda}_s^\nu} / \mathcal{L}. \quad (14)$$

Since \mathcal{W} is not affected by this transformation, the bound (13) can be saturated for any given control path γ by choosing this optimal parameterization. The efficiency then attains its geometric maximum

$$\eta^* = 1 - \mathcal{L}^2/\mathcal{W}\tau. \quad (15)$$

Holding for any thermodynamically consistent microdynamics, our general analysis so far applies to classical and quantum heat engines alike. To explore the fundamental differences between these two regimes, we now model the time evolution of the working medium explicitly using the well-established adiabatic Lindblad approach. This scheme rests on the assumption that the modulations of the system Hamiltonian and the rate at which the external heat source provides thermal energy are both slow compared to the relaxation time of the environment. Applying this condition together with the standard weak-coupling approximation and a coarse-graining in time to wipe out memory effects and fast oscillations yields the Markovian master equation

$$\begin{aligned} \partial_t \rho_t &= \mathbf{L}_{\Lambda_t} \rho_t \quad \text{with} \\ \mathbf{L}_{\Lambda} X &\equiv -\frac{i}{\hbar} [H_{\Lambda}, X] + \sum_{\sigma} \left([V_{\Lambda}^{\sigma} X, V_{\Lambda}^{\sigma\dagger}] + [V_{\Lambda}^{\sigma}, X V_{\Lambda}^{\sigma\dagger}] \right). \end{aligned} \quad (16)$$

Here, \hbar denotes Planck's constant and the Lindblad generator \mathbf{L}_{Λ} depends parametrically on the driving protocols Λ_t , for details see [14, 33–35]. Using (16), the periodic state ρ_t can be determined by means of an adiabatic perturbation theory [36, 37].

This procedure, which we outline in [38], yields the Green-Kubo type expression

$$R_{\Lambda}^{\mu\nu} = -\frac{1}{T} \int_0^{\infty} dt \langle\langle \exp[\mathbf{K}_{\Lambda} t] F_{\Lambda}^{\mu} F_{\Lambda}^{\nu} \rangle\rangle \quad (17)$$

for the adiabatic response coefficients, where the canonical correlation function is defined as

$$\langle\langle X|Y \rangle\rangle \equiv \int_0^1 dx \operatorname{Tr} [\varrho_{\Lambda}^{1-x} X \varrho_{\Lambda}^x Y] - \operatorname{Tr} [\varrho_{\Lambda} X] \operatorname{Tr} [\varrho_{\Lambda} Y] \quad (18)$$

for arbitrary observables X and Y ; the force operators F_{Λ}^{μ} were introduced in (8) and \mathbf{K}_{Λ} denotes the adjoint Lindblad generator, which is defined by the relation $\operatorname{Tr} [X \mathbf{K}_{\Lambda} Y] \equiv \operatorname{Tr} [Y \mathbf{L}_{\Lambda} X]$ [39].

This super operator is subject to three general consistency requirements. First, since we now work on a coarse-grained time scale, where coherent oscillations have been averaged out, the operators V_{Λ}^{σ} can only induce jumps between the energy levels of the working system [35]. Hence, the eigenstates of H_{Λ} form the preferred basis of the dynamics and \mathbf{K}_{Λ} obeys the invariance condition

$$\mathbf{K}_{\Lambda} [H_{\Lambda}, X] = [H_{\Lambda}, \mathbf{K}_{\Lambda} X]. \quad (19)$$

Second, owing to microreversibility, the generators \mathbf{K}_{Λ} and \mathbf{L}_{Λ} are connected by symmetry relation [14]

$$\mathbf{T} \varrho_{\Lambda} \mathbf{K}_{\Lambda} X = \mathbf{L}_{\Lambda} \varrho_{\Lambda} \mathbf{T} X, \quad (20)$$

where the super operator \mathbf{T} induces time reversal [14] and we assume that no magnetic field is applied to the system, i.e., $\mathbf{T} H_{\Lambda} = H_{\Lambda}$ and $\mathbf{T} V_{\Lambda}^{\sigma} = V_{\Lambda}^{\sigma}$. Together with (19), this property implies the adiabatic reciprocity relation $R_{\Lambda}^{\mu\nu} = R_{\Lambda}^{\nu\mu}$, which resembles the familiar Onsager symmetry of linear irreversible thermodynamics [40, 41]. Third, as a technical requirement, we understand that the jump operators V_{Λ}^{σ} form a self-adjoint and irreducible set; this condition ensures that, for Λ fixed, the mean of any observable relaxes to its unique equilibrium value under the dynamics generated by \mathbf{K}_{Λ} in the Heisenberg picture [42]. The expression (17) is then well-defined over the entire space of control parameters.

We are now ready to analyze the impact of quantum effects on slowly driven heat engines from a geometric perspective. To this end, we first divide the mechanical force operator into a diagonal and a coherent part,

$$F_{\Lambda}^w \equiv F_{\Lambda}^d + i[H_{\Lambda}, G_{\Lambda}] \equiv F_{\Lambda}^d + F_{\Lambda}^c. \quad (21)$$

Here, F_{Λ}^d commutes with H_{Λ} and G_{Λ} corresponds to an adiabatic gauge potential [37]. Upon inserting this decomposition into (17), the adiabatic response coefficients decay into two components,

$$R_{\Lambda}^{\mu\nu} = D_{\Lambda}^{\mu\nu} + \delta_{\mu w} \delta_{\nu w} C_{\Lambda}^{ww}, \quad (22)$$

where $D_{\Lambda}^{\mu\nu}$ and C_{Λ}^{ww} are given by the formula (17) with F_{Λ}^w replaced by F_{Λ}^d and F_{Λ}^c , respectively; the cross-terms between F_{Λ}^c and the diagonal operators F_{Λ}^d and F_{Λ}^u vanish due to the property (19) of the adjoint generator. Next, by plugging (22) into the definition (11) of the thermodynamic length and using the concavity of the square-root function, we arrive at the bound [43]

$$\mathcal{L} \geq \sqrt{\mathcal{L}_d^2 + \mathcal{L}_c^2}. \quad (23)$$

The two quantities on the right, which are defined as

$$\mathcal{L}_d \equiv \oint_{\gamma} \sqrt{-D_{\Lambda}^{\mu\nu} d\Lambda^{\mu} d\Lambda^{\nu}} \quad \text{and} \quad \mathcal{L}_c \equiv \oint_{\gamma} \sqrt{-C_{\Lambda}^{ww} d\Lambda^w d\Lambda^w},$$

thereby describe two genuinely different types of energy losses: the reduced thermodynamic length \mathcal{L}_d accounts for the dissipation of heat in the environment and the quantum correction \mathcal{L}_c arises from the decay of superpositions between the energy levels of the working system, a mechanism known as quantum friction [44–48].

The constraint (23) puts an upper limit on the optimal finite-time efficiency (15). This bound,

$$\eta^* \leq 1 - (\mathcal{L}_d^2 + \mathcal{L}_c^2)/\mathcal{W}\tau, \quad (24)$$

which is our second main result, is saturated in the quasi-classical limit, where $F_{\Lambda}^c = 0$; the energy eigenstates of the system are then time-independent and the periodic state ρ_t is diagonal in this basis throughout the cycle. In fact, since the adiabatic work \mathcal{W} is independent of F_{Λ}^c ,

the bound (24) shows that injecting coherence into the working system can only reduce the maximum efficiency of the engine at given power. These coherence-induced performance losses are a universal feature of the slow-driving regime, where superpositions between different energy levels are irreversibly destroyed by the environment before their work content can be extracted through mechanical operations. While similar conclusions were drawn before for specific models [44–48] and small driving amplitudes [14, 49], our new bound (24) applies to any heat engine that is covered by Lindblad dynamics and operated in adiabatic response. Thus, it further corroborates the emerging picture that quantum effects can enhance the performance of thermal machines only far from equilibrium [49–51].

We will now show how our general results can be applied to practical devices. To this end, we consider a simple model for a solid-state quantum heat engine that is inspired by a recent experiment [7]. The working system consists of a superconducting qubit with Hamiltonian

$$H_\lambda = -\frac{\hbar\Omega}{2}(\varepsilon\sigma_x + \sqrt{\lambda^2 - \varepsilon^2}\sigma_z). \quad (25)$$

Here, σ_x and σ_z are the usual Pauli matrices, $\hbar\Omega$ denotes the overall energy scale and the dimensionless parameters $\varepsilon \geq 0$ and $\lambda \geq \varepsilon$ correspond to the tunneling energy and the flux-tunable level-splitting of the qubit [52, 53]. The role the environment is played by a normal-metal island, whose temperature can be accurately controlled with established techniques [54] and monitored by means of sensitive electron thermometers, a technology that could soon enable calorimetric work measurements [55–60]. This reservoir can be described in terms of two jump operators, V_Λ^+ and V_Λ^- , defined by the conditions

$$[H_\lambda, V_\Lambda^\pm] = \pm\hbar\Omega\lambda V_\Lambda^\pm, \quad \text{Tr}[V_\Lambda^\pm V_\Lambda^{\pm\dagger}] = \frac{\pm\Gamma\Omega\lambda}{1 - \exp[\mp\hbar\Omega\lambda/T]},$$

where Γ determines the average jump frequency.

We proceed in three steps. First, we evaluate the adiabatic response coefficients for the single-qubit engine using the formula (17). Second, we calculate the geometric quantities entering the bounds (13) and (24) and the optimal speed function ϕ_t defined in (14). For simplicity, we thereby assume that the device is driven by harmonic temperature and energy modulations, i.e., we set

$$\Lambda_t = (\hbar\Omega(1 + \sin^2[\pi\Omega t]), 1 + \sin^2[\pi\Omega t + \pi/4]). \quad (26)$$

Hence, the control path γ is a circle in the $\Lambda^u - \Lambda^w$ plane. Third, in order to assess the quality of our bounds, we determine the periodic state ρ_t of the system exactly by solving the time-inhomogeneous master equation (16) for both constant and optimal driving speed. Using the expressions (2) and (3), the power and the efficiency of the engine can thus be obtained for any cycle time τ .

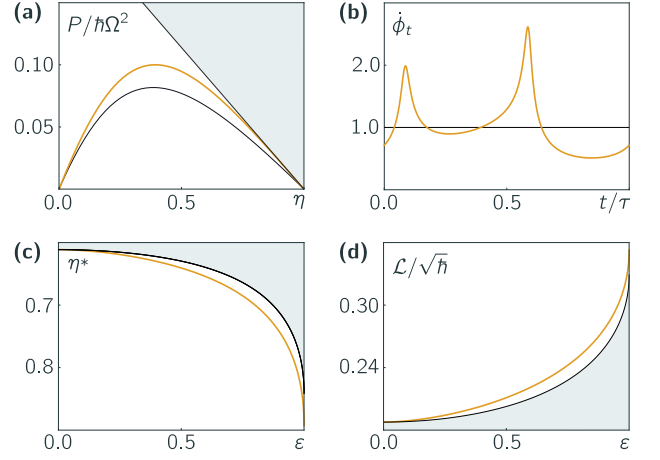


FIG. 2. Performance of a single-qubit engine. Upper panel: Geometric optimization. Plot (a) shows how the average power of the engine behaves compared to its efficiency when the cycle time is varied from $\tau = 1/10\Omega$ to $\tau = 50/\Omega$ for $\varepsilon = 3/5$. The two curves are obtained for linear (black) and optimal (orange) parameterization of the control path; the derivatives of the corresponding speed functions are shown in (b). The shaded area in (a) is inaccessible in adiabatic response by virtue of our bound (13). Lower panel: Quantum losses. The orange curves show the optimal efficiency (15) for $\tau = 3/\Omega$ (c) and the thermodynamic length (d) as a function of the coherence parameter ε ; shaded areas indicate the bounds (24) and (23). For all plots, we have set $\Gamma = 5$.

The results of this analysis are summarized in Fig. 2, for details see [38]. We find that, for optimal driving speed, our bound (13) is practically attained in the range $\eta \gtrsim 0.8$, which corresponds to $\tau \gtrsim 2/\Omega$. The optimal protocols $\Lambda_t^* \equiv \Lambda_{\phi_t}$ thereby outperform the harmonic profiles (26) by roughly a factor 1.2 in power at given efficiency. Remarkably, this increase in performance persists even for $\eta < 0.8$, i.e., for short cycle times $\tau < 2/\Omega$, which are not covered by the slow-driving approximation (9). This phenomenon, whose degree of universality is yet to be established, raises the appealing perspective that it might be possible to extend our geometric description of microscopic heat engines beyond the limits of adiabatic response.

The lower panel of Fig. 2 shows that the single-qubit engine operates most efficiently in the quasi-classical configuration $\varepsilon = 0$. For this setting, the eigenstates of the Hamiltonian (25) are independent of λ and our bounds (23) and (24) are saturated. Raising the value of ε leads to increasing quantum friction. Hence, the thermodynamic length grows and the optimal efficiency drops, whereby both figures closely follow their upper and lower bound, respectively. This behavior underlines our general result that coherence only reduces the efficiency of thermodynamic cycles in adiabatic response. Although this conclusion does not extend to the fast-driving regime, it still provides a valuable guideline for future theoretical and experimental studies seeking new strategies to gain a quantum advantage in the design of thermal machines.

K.B. thanks P. Menczel for insightful discussions and for a careful proof reading of this manuscript and J. P. Pekola for helpful comments. K.B. acknowledges support from Academy of Finland (Contract No. 296073) and is associated with the Centre for Quantum Engineering at Aalto University. K.S. was supported by JSPS Grants-in-Aid for Scientific Research (JP17K05587, JP16H02211).

-
- [1] V. Blickle and C. Bechinger, “Realization of a micrometer-sized stochastic heat engine,” *Nature Phys.* **8**, 143 (2011).
- [2] I. A. Martínez, É. Roldán, L. Dinis, D. Petrov, J. M. R. Parrondo, and R. A. Rica, “Brownian Carnot engine,” *Nature Phys.* **12**, 67 (2015).
- [3] I. A. Martínez, É. Roldán, L. Dinis, D. Petrov, and R. A. Rica, “Adiabatic Processes Realized with a Trapped Brownian Particle,” *Phys. Rev. Lett.* **114**, 120601 (2015).
- [4] O. Abah, J. Roßnagel, G. Jacob, S. Deffner, F. Schmidt-Kaler, K. Singer, and E. Lutz, “Single-Ion Heat Engine at Maximum Power,” *Phys. Rev. Lett.* **109**, 203006 (2012).
- [5] J. Roßnagel, S. T. Dawkins, K. N. Tolazzi, O. Abah, E. Lutz, F. Schmidt-Kaler, and K. Singer, “A single-atom heat engine,” *Science* **352**, 325 (2016).
- [6] J. Klatzow, J. N. Becker, P. M. Ledingham, C. Weinzel, K. T. Kaczmarek, D. J. Saunders, J. Nunn, I. A. Walmsley, R. Uzdin, and E. Poem, “Experimental Demonstration of Quantum Effects in the Operation of Microscopic Heat Engines,” *Phys. Rev. Lett.* **122**, 110601 (2017).
- [7] A. Ronzani, B. Karimi, J. Senior, Y.-C. Chang, J. T. Peltonen, C. D. Chen, and J. P. Pekola, “Tunable photonic heat transport in a quantum heat valve,” *Nat. Phys.* (2018), 10.1038/s41567-018-0199-4.
- [8] Bjarne Andresen, “Current trends in finite-time thermodynamics,” *Angew. Chem. Int. Ed.* **50**, 2690 (2011).
- [9] G. Benenti, K. Saito, and G. Casati, “Thermodynamic Bounds on Efficiency for Systems with Broken Time-Reversal Symmetry,” *Phys. Rev. Lett.* **106**, 230602 (2011).
- [10] K. Brandner, K. Saito, and U. Seifert, “Thermodynamics of Micro- and Nano-Systems Driven by Periodic Temperature Variations,” *Phys. Rev. X* **5**, 031019 (2015).
- [11] K. Brandner and U. Seifert, “Bound on thermoelectric power in a magnetic field within linear response,” *Phys. Rev. E* **91**, 012121 (2015).
- [12] K. Proesmans and C. Van den Broeck, “Onsager Coefficients in Periodically Driven Systems,” *Phys. Rev. Lett.* **115**, 090601 (2015).
- [13] K. Proesmans, B. Cleuren, and C. Van den Broeck, “Power-Efficiency-Dissipation Relations in Linear Thermodynamics,” *Phys. Rev. Lett.* **116**, 220601 (2016).
- [14] K. Brandner and U. Seifert, “Periodic thermodynamics of open quantum systems,” *Phys. Rev. E* **93**, 062134 (2016).
- [15] N. Shiraishi, K. Saito, and H. Tasaki, “Universal Trade-Off Relation between Power and Efficiency for Heat Engines,” *Phys. Rev. Lett.* **117**, 190601 (2016).
- [16] P. Pietzonka and U. Seifert, “Universal Trade-Off between Power, Efficiency, and Constancy in Steady-State Heat Engines,” *Phys. Rev. Lett.* **120**, 190602 (2018).
- [17] N. Shiraishi and K. Saito, “Fundamental Relation Between Entropy Production and Heat Current,” *J. Stat. Phys.* **174**, 433 (2019).
- [18] G. Ruppeiner, “Riemannian geometry in thermodynamic fluctuation theory,” *Rev. Mod. Phys.* **67**, 605 (1995).
- [19] B. Andresen, P. Salamon, and R. S. Berry, “Thermodynamics in finite time,” *Phys. Today* **37**, 62 (1984).
- [20] D. Brody and N. Rivier, “Geometrical aspects of statistical mechanics,” *Phys. Rev. E* **51**, 1006 (1995).
- [21] G. E. Crooks, “Measuring Thermodynamic Length,” *Phys. Rev. Lett.* **99**, 100602 (2007).
- [22] S. Deffner and E. Lutz, “Thermodynamic length for far-from-equilibrium quantum systems,” *Phys. Rev. E* **87**, 022143 (2013).
- [23] M. Scandi and M. Perarnau-Llobet, “Thermodynamic length in open quantum systems,” preprint (2018), arXiv:1810.05583.
- [24] P. R. Zulkowski, D. A. Sivak, G. E. Crooks, and M. R. DeWeese, “Geometry of thermodynamic control,” *Phys. Rev. E* **86**, 041148 (2012).
- [25] D. A. Sivak and G. E. Crooks, “Thermodynamic Metrics and Optimal Paths,” *Phys. Rev. Lett.* **108**, 190602 (2012).
- [26] G. M. Rotskoff and G. E. Crooks, “Optimal control in nonequilibrium systems : Dynamic Riemannian geometry of the Ising model,” *Phys. Rev. E* **92**, 060102 (2015).
- [27] B. Machta, “Dissipation Bound for Thermodynamic Control,” *Phys. Rev. Lett.* **115**, 260603 (2015).
- [28] P. Salamon and R. S. Berry, “Thermodynamic Length and Dissipated Availability,” *Phys. Rev. Lett.* **51**, 1127 (1983).
- [29] To this end, observe that the first law, $\dot{E}_t = J_t - P_t$, implies $-f_t^\mu \dot{\Lambda}_t^\mu = T_t \Sigma_t + \partial_t (E_t - T_t S_t)$ and that $\Sigma_t \equiv \dot{S}_t - J_t/T_t \geq 0$ corresponds to the total rate of entropy production. Here, E_t and $S_t = f_t^\mu$ denote the internal energy and entropy of the system, respectively, J_t is the rate of heat uptake from the environment and P_t the instantaneous power.
- [30] Specifically, we have $\eta_{th}/\eta_C \equiv W/Q\eta_C \leq \eta$, where Q denotes the heat uptake during the hot phase, $\eta_C \equiv 1 - T_c/T_h$ is the Carnot factor and T_h and $T_c < T_h$ correspond to the hot and the cold temperature.
- [31] L. D’Alessio and A. Polkovnikov, “Emergent Newtonian dynamics and the geometric origin of mass,” *Ann. Phys.* **345**, 141 (2014).
- [32] Note that the matrix $g_{\Lambda}^{\mu\nu}$ must be positive semi-definite, since the second law requires $A \geq 0$ for any closed path γ and any parameterization.
- [33] R. Alicki, “The quantum open system as a model of the heat engine,” *J. Phys. A: Math. Gen.* **12**, L103 (1979).
- [34] T. Albash, S. Boixo, D. A. Lidar, and P. Zanardi, “Quantum adiabatic Markovian master equations,” *New J. Phys.* **14**, 123016 (2012).
- [35] C. Majenz, T. Albash, H.-P. Breuer, and D. A. Lidar, “Coarse graining can beat the rotating-wave approximation in quantum Markovian master equations,” *Phys. Rev. A* **88**, 012103 (2013).
- [36] V. Cavina, A. Mari, and V. Giovannetti, “Slow Dynamics and Thermodynamics of Open Quantum Systems,” *Phys. Rev. Lett.* **119**, 050601 (2017).
- [37] P. Weinberg, M. Bukov, L. D’Alessio, A. Polkovnikov, S. Vajna, and M. Kolodrubetz, “Adiabatic perturbation theory and geometry of periodically-driven systems,”

- Phys. Rep.* **688**, 1 (2017).
- [38] “Supplemental Material,” URL.
- [39] Specifically, the adjoint Lindblad generator is given by $K_\Lambda X \equiv \frac{i}{\hbar} [H_\lambda, X] + \sum_\sigma (V_\Lambda^{\sigma\dagger} [X, V_\Lambda^\sigma] + [V_\Lambda^{\sigma\dagger}, X] V_\Lambda^\sigma)$.
- [40] L. Onsager, “Reciprocal relations in irreversible processes I,” *Phys. Rev.* **37**, 405 (1931).
- [41] L. Onsager, “Reciprocal relations in irreversible processes II,” *Phys. Rev.* **38**, 2265 (1931).
- [42] H. Spohn, “An algebraic condition for the approach to equilibrium of an open N-level system,” *Lett. Math. Phys.* **2**, 33 (1977).
- [43] To derive (23), observe that $\mathcal{L} \geq \sqrt{\alpha} \mathcal{L}_d + \sqrt{1-\alpha} \mathcal{L}_c$ for $0 \leq \alpha \leq 1$ by the concavity of the square root function. Maximizing the right-hand side of this inequality with respect to α yields the desired result.
- [44] R. Kosloff and T. Feldmann, “Discrete four-stroke quantum heat engine exploring the origin of friction,” *Phys. Rev. E* **65**, 055102(R) (2002).
- [45] T. Feldmann and R. Kosloff, “Quantum four-stroke heat engine: Thermodynamic observables in a model with intrinsic friction,” *Phys. Rev. E* **68**, 016101 (2003).
- [46] T. Feldmann and R. Kosloff, “Characteristics of the limit cycle of a reciprocating quantum heat engine,” *Phys. Rev. E* **70**, 046110 (2004).
- [47] T. Feldmann and R. Kosloff, “Quantum lubrication: Suppression of friction in a first-principles four-stroke heat engine,” *Phys. Rev. E* **73**, 025107(R) (2006).
- [48] T. Feldmann and R. Kosloff, “Short time cycles of purely quantum refrigerators,” *Phys. Rev. E* **85**, 051114 (2012).
- [49] K. Brandner, M. Bauer, and U. Seifert, “Universal Coherence-Induced Power Losses of Quantum Heat Engines in Linear Response,” *Phys. Rev. Lett.* **119**, 170602 (2017).
- [50] R. Uzdin, A. Levy, and R. Kosloff, “Equivalence of Quantum Heat Machines, and Quantum-Thermodynamic Signatures,” *Phys. Rev. X* **5**, 031044 (2015).
- [51] R. Uzdin, “Coherence-Induced Reversibility and Collective Operation of Quantum Heat Machines via Coherence Recycling,” *Phys. Rev. Appl.* **6**, 024004 (2016).
- [52] A. O. Niskanen, Y. Nakamura, and J. P. Pekola, “Information entropic superconducting microcooler,” *Phys. Rev. B* **76**, 174523 (2007).
- [53] B. Karimi and J. P. Pekola, “Otto refrigerator based on a superconducting qubit - classical and quantum performance,” *Phys. Rev. B* **94**, 184503 (2016).
- [54] F. Giazotto, T. T. Heikkilä, A. Luukanen, A. M. Savin, and J. P. Pekola, “Opportunities for mesoscopes in thermometry and refrigeration: Physics and applications,” *Rev. Mod. Phys.* **78**, 217 (2006).
- [55] M. Campisi, J. P. Pekola, and R. Fazio, “Nonequilibrium fluctuations in quantum heat engines: theory, example, and possible solid state experiments,” *New J. Phys.* **17**, 035012 (2015).
- [56] K. L. Viisanen, S. Suomela, S. Gasparinetti, O.-P. Saira, J. Ankerhold, and J. P. Pekola, “Incomplete measurement of work in a dissipative two level system,” *New J. Phys.* **17**, 055014 (2015).
- [57] S. Gasparinetti, K. L. Viisanen, O.-P. Saira, T. Faivre, M. Arzeo, M. Meschke, and J. P. Pekola, “Fast Electron Thermometry for Ultrasensitive Calorimetric Detection,” *Phys. Rev. Appl.* **3**, 014007 (2015).
- [58] A. Kupiainen, P. Muratore-Ginanneschi, J. Pekola, and K. Schwieger, “Fluctuation relation for qubit calorimetry,” *Phys. Rev. E* **94**, 062127 (2016).
- [59] B. Donvil, P. Muratore-Ginanneschi, J. P. Pekola, and K. Schwieger, “Model for calorimetric measurements in an open quantum system,” *Phys. Rev. A* **97**, 052107 (2018).
- [60] L. B. Wang, O.P. Saira, and J. P. Pekola, “Fast thermometry with a proximity Josephson junction,” *Appl. Phys. Lett.* **112**, 013105 (2018).

Thermodynamic Geometry of Microscopic Heat Engines: Supplemental Material

I. LINDBLAD DYNAMICS AND ADIABATIC RESPONSE THEORY

In this section, we provide a brief technical review of the adiabatic Lindblad approach to the dynamics of slowly driven open quantum systems, which is based on [1] and the references therein. We then derive the expression Eq. (17) for the adiabatic response coefficients and discuss the general properties of these quantities.

A. Framework

In the adiabatic Lindblad scheme, the time evolution of the state ρ_t of the working system is governed by the Markovian master equation

$$\partial_t \rho_t = \mathcal{L}_t \rho_t \equiv (-i\mathcal{H}_t + \mathcal{D}_t) \rho_t. \quad (1)$$

Here, the two super operators

$$\begin{aligned} \mathcal{H}X &\equiv [H, X]/\hbar \quad \text{and} \\ \mathcal{D}X &\equiv \sum_{\sigma} ([V^{\sigma} X, V^{\sigma\dagger}] + [V^{\sigma}, X V^{\sigma\dagger}]) \end{aligned} \quad (2)$$

describe the unitary dynamics of the bare system and the influence of the environment, respectively. Note that, for convenience, we notationally suppress the dependence of super operators, operators and scalar quantities on the control parameters Λ throughout this section; to indicate explicit dependence on the driving protocols Λ_t , we use the abbreviations $X_{\Lambda_t} \equiv X_t$ and $X_{\Lambda_t} \equiv X_t$.

Owing to micro-reversibility, the dissipation super operator introduced in (2) has to obey the quantum detailed balance condition

$$\varrho \mathcal{D}^{\dagger} X = \mathcal{D} \varrho X. \quad (3)$$

Here, ϱ denotes the thermal state defined in Eq. (6) and the adjoint of \mathcal{D} with respect to the Hilbert-Schmidt scalar product is given by

$$\mathcal{D}^{\dagger} X \equiv \sum_{\sigma} (V^{\sigma\dagger} [X, V^{\sigma}] + [V^{\sigma\dagger}, X] V^{\sigma}). \quad (4)$$

This relation has two important consequences. First, it implies the commutation rules

$$\mathcal{H}\mathcal{D} = \mathcal{D}\mathcal{H} \quad \text{and} \quad \mathcal{H}\mathcal{D}^{\dagger} = \mathcal{D}^{\dagger}\mathcal{H}, \quad (5)$$

where the second identity is equivalent to the invariance condition Eq. (19), since $\mathcal{K} = i\mathcal{H} + \mathcal{D}^{\dagger}$. Second, as a result of (3), the two super operators \mathcal{H} and \mathcal{D} are both self-adjoint with respect to the scalar product

$$\langle X|Y \rangle \equiv \int_0^1 dx \operatorname{Tr}[\varrho^{1-x} X^{\dagger} \varrho^x Y] \quad (6)$$

in the operator space of the working system. Hence, there exists a joint set of normalized eigenvectors M^j satisfying

$$\mathcal{H}M^j = \omega^j M^j, \quad \mathcal{D}^{\dagger}M^j = \kappa^j M^j, \quad \langle M^j|M^k \rangle = \delta_{jk},$$

where the eigenvalues ω^j and κ^j are real and $\kappa^j \leq 0$. Moreover, if the set of jump operators V^{σ} is self-adjoint and irreducible, we have $\kappa^0 = 0$ and $\kappa^j < 0$ for $j > 0$, where $M^0 = \mathbb{1}$ is the unique stationary eigenvector of \mathcal{D}^{\dagger} .

B. Adiabatic Response Coefficients

The formula Eq. (17) can now be derived by solving the master equation (1) in the slow-driving regime using adiabatic perturbation theory [2, 3]. To this end, we apply the ansatz

$$\rho_t = \varrho_t + \int_0^1 dx \varrho_t^{1-x} \xi_t \varrho_t^x, \quad (7)$$

where ξ_t is understood to be a small perturbation of first order in the driving rates $\dot{\Lambda}_t$. Inserting (7) into (1), using the relations (3) and (5) and neglecting higher-order corrections yields the algebraic equation

$$(-i\mathcal{H}_t + \mathcal{D}_t^{\dagger})\xi_t = (F_t^{\mu} - \langle \mathbb{1}|F_t^{\mu} \rangle)\dot{\Lambda}_t^{\mu}/T_t. \quad (8)$$

Since we assume that $M^0 = \mathbb{1}$ is the only stationary eigenvector of \mathcal{D}^{\dagger} , the operator on the right of (8) is orthogonal to the nullspace of the super operator acting on ξ_t on the left. Hence, the unique solution of (8) reads

$$\xi_t = -\frac{1}{T} \int_0^{\infty} ds \exp[(-i\mathcal{H}_t + \mathcal{D}_t^{\dagger})s] (F_t^{\mu} - \langle \mathbb{1}|F_t^{\mu} \rangle) \dot{\Lambda}_t^{\mu}. \quad (9)$$

Upon inserting this result into (7), using the definition Eq. (3) of the thermodynamic forces and neglecting higher-order terms in the driving rates, we arrive at

$$\begin{aligned} f_t^{\mu} - \langle \mathbb{1}|F_t^{\mu} \rangle &= -\frac{1}{T} \int_0^{\infty} ds \langle (F_t^{\nu} - \langle \mathbb{1}|F_t^{\nu} \rangle) | \exp[\mathcal{K}_t s] F_t^{\mu} \rangle \dot{\Lambda}_t^{\nu} \\ &= -\frac{1}{T} \int_0^{\infty} ds \langle \exp[\mathcal{K}_t s] F_t^{\mu} | (F_t^{\nu} - \langle \mathbb{1}|F_t^{\nu} \rangle) \rangle \dot{\Lambda}_t^{\nu} \\ &= -\frac{1}{T} \int_0^{\infty} ds \langle \langle \exp[\mathcal{K}_t s] F_t^{\mu} | F_t^{\nu} \rangle \rangle \dot{\Lambda}_t^{\nu}. \end{aligned} \quad (10)$$

Here, we have used that $\mathcal{K} = i\mathcal{H} + \mathcal{D}^{\dagger}$ in the first line; the second line follows by noting $\langle X|Y \rangle = \langle Y|X \rangle^* = \langle Y^{\dagger}|X^{\dagger} \rangle$ and $(\mathcal{K}X)^{\dagger} = \mathcal{K}X^{\dagger}$; in the last line, we have inserted the definition Eq. (18) of the canonical correlation function. Finally, observing that $\langle \mathbb{1}|F_t^{\mu} \rangle = \mathcal{F}_t^{\mu}$ and comparing the last line of (10) with Eq. (9) yields the result Eq. (17).

We now observing that Eq. (17) can be rewritten as

$$\begin{aligned} R^{\mu\nu} &= -\frac{1}{T} \int_0^{\infty} dt \langle \exp[\mathcal{K}t] \delta F^{\mu} | \delta F^{\nu} \rangle \quad \text{with} \\ \delta F^{\mu} &\equiv F^{\mu} - \langle \mathbb{1}|F^{\mu} \rangle. \end{aligned} \quad (11)$$

Using this expression, the three key properties of the coefficients Eq. (17), i.e., the positivity of the metric $g^{\mu\nu} = -(R^{\mu\nu} + R^{\nu\mu})/2$, the reciprocity relation $R^{\mu\nu} = R^{\nu\mu}$ and the decomposition law Eq. (22), can be derived in a straightforward manner as we show in the following.

1 - *Positivity*. For arbitrary real variables h_μ , we have

$$\begin{aligned} Tg^{\mu\nu}h_\mu h_\nu &= -\int_0^\infty dt \langle \exp[\mathbf{K}t] \delta F^h | \delta F^h \rangle \\ &= -\int_0^\infty dt \langle \delta F^h | (\exp[\mathbf{K}t] + \exp[\tilde{\mathbf{K}}t]) \delta F^h \rangle / 2 \\ &= -\sum_{j>0} \kappa^j |\langle M^j | \delta F^h \rangle|^2 / |\kappa^j + i\omega^j|^2 \geq 0. \end{aligned} \quad (12)$$

Here, we have defined $\delta F^h \equiv h_\mu \delta F^\mu$ in the first line; the second line is obtained by observing

$$\begin{aligned} \langle \mathbf{K}X | X \rangle &= \langle X | \tilde{\mathbf{K}}X \rangle \quad \text{and} \\ \langle \mathbf{K}X | X \rangle &= \langle X | \mathbf{K}X \rangle^* = \langle X^\dagger | (\mathbf{K}X)^\dagger \rangle = \langle X^\dagger | \mathbf{K}X^\dagger \rangle, \end{aligned} \quad (13)$$

where $\tilde{\mathbf{K}} \equiv -i\mathbf{H} + \mathbf{D}^\dagger$; the third line in (12) follows by expanding δF^h in the joint eigenvectors of \mathbf{H} and \mathbf{D} .

2 - *Reciprocity Relations*. For systems without a magnetic field, the generators \mathbf{K} and \mathbf{L} obey the symmetry relation Eq. (20), which is equivalent to

$$\mathbf{T}\mathbf{K} = \tilde{\mathbf{K}}\mathbf{T} \quad (14)$$

by virtue of (3). Here, $\mathbf{T}X = \Theta X \Theta^{-1}$ and Θ denotes the anti-unitary time-reversal operator. Hence, we have

$$\langle \mathbf{K}\mathbf{T}X | \mathbf{T}Y \rangle = \langle \mathbf{T}X | \tilde{\mathbf{K}}\mathbf{T}Y \rangle = \langle X^\dagger | \mathbf{T}^{-1} \tilde{\mathbf{K}}\mathbf{T}Y^\dagger \rangle = \langle X^\dagger | \mathbf{K}Y^\dagger \rangle.$$

Applying this identity to (11) and noting that $\mathbf{T}F^\mu = F^\mu$ for time-reversal symmetric systems yields the reciprocity relation $R^{\mu\nu} = R^{\nu\mu}$.

3 - *Decomposition*. Note that Eq. (21) is equivalent to

$$\delta F^w = \delta F^d + i\mathbf{H}\mathbf{G} = \delta F^d + F^c. \quad (15)$$

Inserting this line into (11), recalling that \mathbf{H} commutes with \mathbf{K} and that $\mathbf{H}\delta F^d = \mathbf{H}\delta F^u = 0$ yields the decomposition law Eq. (22).

II. SINGLE-QUBIT HEAT ENGINE

We provide further details on the example discussed in the last part of the main text. Specifically, we first show how to determine the geometric properties of this system and then explain how its finite-time thermodynamics can be analyzed beyond the adiabatic response regime.

A. Geometric Quantities

We first observe that the Hamiltonian Eq. (25) can be decomposed as

$$H_\lambda = \frac{\hbar\Omega\lambda}{2} (|E_\lambda^+\rangle\langle E_\lambda^+| - |E_\lambda^-\rangle\langle E_\lambda^-|), \quad (16)$$

where the normalized eigenvectors are given by

$$|E_\lambda^+\rangle = \begin{pmatrix} \sin[\theta_\lambda/2] \\ -\cos[\theta_\lambda/2] \end{pmatrix} \quad \text{and} \quad |E_\lambda^-\rangle = \begin{pmatrix} \cos[\theta_\lambda/2] \\ \sin[\theta_\lambda/2] \end{pmatrix} \quad \text{with} \quad \sin[\theta_\lambda/2] \equiv \varepsilon / \sqrt{2\lambda^2 + 2\lambda\sqrt{\lambda^2 - \varepsilon^2}}. \quad (17)$$

Furthermore, the free energy and the adiabatic forces Eq. (7) for the qubit are given by

$$\begin{aligned} \mathcal{F}_\Lambda &= -T \ln[2 \cosh[\hbar\Omega\lambda/2T]], \\ \mathcal{F}_\Lambda^u &= -\mathcal{F}_\Lambda/T - (\hbar\Omega\lambda/2T) \tanh[\hbar\Omega\lambda/2T] \quad \text{and} \\ \mathcal{F}_\Lambda^w &= (\hbar\Omega/2) \tanh[\hbar\Omega\lambda/2T]. \end{aligned} \quad (18)$$

Using this result, the geometric work for an arbitrary engine cycle becomes

$$\mathcal{W} = \int_0^\tau dt \mathcal{F}_{\Lambda_t}^w \dot{\Lambda}_t^w = \frac{\hbar\Omega}{2} \int_0^\tau dt \tanh[\hbar\Omega\lambda_t/2T_t] \dot{\lambda}_t. \quad (19)$$

Note that this expression is independent of the coherence parameter ε .

For the remaining geometric quantities, we have to evaluate the adiabatic response coefficients Eq. (17). To this end, we proceed in three steps. First, we note that the jump operators defined in the main text are given by

$$V_\Lambda^\pm = \sqrt{\frac{\pm\Gamma\Omega\lambda}{1 - \exp[\mp\hbar\Omega\lambda/T]}} (\Pi_\lambda^x \pm i\Pi_\lambda^y)/2, \quad (20)$$

where

$$\begin{aligned} \Pi_\lambda^x &\equiv |E_\lambda^+\rangle\langle E_\lambda^-| + |E_\lambda^-\rangle\langle E_\lambda^+|, \quad \Pi_\lambda^y \equiv i|E_\lambda^-\rangle\langle E_\lambda^+| - i|E_\lambda^+\rangle\langle E_\lambda^-|, \\ \Pi_\lambda^z &\equiv |E_\lambda^+\rangle\langle E_\lambda^+| - |E_\lambda^-\rangle\langle E_\lambda^-|. \end{aligned}$$

The super operators $\mathbf{D}_\Lambda^\dagger$ and \mathbf{H}_λ thus share the normalized eigenvectors

$$\begin{aligned} M_\Lambda^0 &= \mathbb{1}, \\ M_\Lambda^z &= \cosh[\hbar\Omega\lambda/2T] \Pi_\lambda^z + \sinh[\hbar\Omega\lambda/2T] \mathbb{1} \quad \text{and} \\ M_\Lambda^\pm &= \sqrt{\frac{\hbar\Omega\lambda}{T \tanh[\hbar\Omega\lambda/2T]}} (\Pi_\lambda^x \pm i\Pi_\lambda^y)/2 \end{aligned} \quad (21)$$

with corresponding eigenvalues

$$\begin{aligned} \kappa_\Lambda^0 &= 0, \quad \kappa_\Lambda^z = -2\Gamma\Omega\lambda \coth[\hbar\Omega\lambda/2T], \quad \kappa_\Lambda^\pm = \kappa_\Lambda^z/2, \\ \omega_\lambda^0 &= \omega_\lambda^z = 0, \quad \omega_\lambda^\pm = \pm\Omega\lambda. \end{aligned} \quad (22)$$

Second, we calculate the shifted force operators

$$\delta F_\Lambda^u \equiv F_\Lambda^u - \mathcal{F}_\Lambda^u = \frac{\hbar\Omega\lambda}{2T \cosh[\hbar\Omega\lambda/2T]} M_\Lambda^z \quad \text{and} \quad (23)$$

$$\delta F_\Lambda^w = \delta F_\Lambda^d + F_\Lambda^c \quad \text{with}$$

$$\delta F_\Lambda^d \equiv F_\Lambda^d - \mathcal{F}_\Lambda^w = -\frac{\hbar\Omega}{2 \cosh[\hbar\Omega\lambda/2T]} M_\Lambda^z \quad \text{and}$$

$$F_\Lambda^c \equiv \frac{\varepsilon \sqrt{\hbar\Omega\lambda T \tanh[\hbar\Omega\lambda/2T]}}{2\lambda\sqrt{\lambda^2 - \varepsilon^2}} (M_\Lambda^+ + M_\Lambda^-),$$

see Eq. (8) and Eq. (21) for the general definitions of F_{Λ}^{μ} , F_{Λ}^d and F_{Λ}^c . Third, upon inserting (23) into (11) and recalling that the operators (22) are eigenvectors of the generator K_{Λ} , we arrive at

$$\begin{pmatrix} R_{\Lambda}^{uu} & R_{\Lambda}^{uw} \\ R_{\Lambda}^{wu} & R_{\Lambda}^{ww} \end{pmatrix} = \begin{pmatrix} -\lambda/T^3 & 1/T^2 \\ 1/T^2 & -1/\lambda T \end{pmatrix} \mathcal{R}_{\Lambda} + \begin{pmatrix} 0 & 0 \\ 0 & C_{\Lambda}^{ww} \end{pmatrix} \quad (24)$$

and $D_{\Lambda}^{ww} = R_{\Lambda}^{ww} - C_{\Lambda}^{ww}$ with

$$C_{\Lambda}^{ww} = -\frac{\hbar \varepsilon^2}{2\lambda^2(\lambda^2 - \varepsilon^2)} \frac{\Gamma}{\Gamma^2 \coth^2[\hbar\Omega\lambda/2T] + 1}, \quad (25)$$

$$\mathcal{R}_{\Lambda} \equiv \frac{\hbar^2 \Omega}{8\Gamma} \frac{\tanh[\hbar\Omega\lambda/2T]}{\cosh^2[\hbar\Omega\lambda/2T]}.$$

The quantities \mathcal{L} , \mathcal{L}_d and \mathcal{L}_d are now obtained by inserting (24) and the protocols Eq. (26) into the corresponding definitions of the main text and carrying out the remaining integrals numerically. To determine the optimal speed function ϕ_t , we evaluate the expression

$$\phi_{t_k}^{-1} = \tau \int_0^{t_k} ds \sqrt{g_{\Lambda_s}^{\mu\nu} \dot{\Lambda}_s^{\mu} \dot{\Lambda}_s^{\nu}} / \mathcal{L}, \quad (26)$$

which is equivalent to Eq. (14), for a sufficiently large number of sampling points $0 \leq t_k \leq \tau$ and determine the discretized speed function ϕ_{t_k} by point-wise inversion; the continuous function ϕ_t is recovered by interpolation.

B. Exact Dynamics

To analyze the performance of the single-qubit engine without the adiabatic approximation Eq. (9), we have to

solve the master equation

$$\partial_t \rho_t = \mathcal{L}_{\Lambda_t} \rho_t. \quad (27)$$

To this end, it is convenient to parameterized the periodic state ρ_t in the form

$$\rho_t \equiv \mathbb{1}/2 + r_t^x \Pi_{\lambda_t}^x + r_t^y \Pi_{\lambda_t}^y + r_t^z \Pi_{\lambda_t}^z. \quad (28)$$

Plugging this ansatz in into (27) yields the generalized Bloch equations

$$\partial_t \begin{pmatrix} r_t^x \\ r_t^y \\ r_t^z \end{pmatrix} = \begin{pmatrix} -k_{\Lambda_t}^+ & -\Omega \lambda_t & -\theta'_{\lambda_t} \dot{\lambda}_t \\ \Omega \lambda_t & -k_{\Lambda_t}^+ & 0 \\ \theta'_{\lambda_t} \dot{\lambda}_t & 0 & -2k_{\Lambda_t}^+ \end{pmatrix} \begin{pmatrix} r_t^x \\ r_t^y \\ r_t^z \end{pmatrix} + \begin{pmatrix} 0 \\ 0 \\ k_{\Lambda_t}^- \end{pmatrix} \quad (29)$$

with

$$k_{\Lambda}^{\pm} \equiv \Gamma \Omega \lambda \frac{1 \pm \exp[\hbar\Omega\lambda/T]}{\exp[\hbar\Omega\lambda/T] - 1} \quad \text{and} \quad \theta'_{\lambda} \equiv \frac{\varepsilon}{\lambda \sqrt{\lambda^2 - \varepsilon^2}}. \quad (30)$$

After inserting a specific set of driving protocols, i.e., for the setup discussed in the main text, either the harmonic profiles Eq. (26) of the corresponding optimal protocols $\Lambda_t^* = \Lambda_{\phi_t}$, the differential equations (29) have to be solved numerically with respect to periodic boundary conditions. The exact input and output of the engine can then be determined by evaluating the expressions

$$W = -\hbar\Omega \int_0^{\tau} dt (\lambda_t \theta'_{\lambda_t} r_t^x + r_t^z) \dot{\lambda}_t \quad \text{and} \quad (31)$$

$$U = \frac{1}{2} \int_0^{\tau} dt (4r_t \operatorname{arctanh}[2r_t] + \ln[1/4 - r_t^2]) \dot{I}_t,$$

which follow directly from Eq. (2). Note that we have used the short-hand notation $r_t \equiv \sqrt{(r_t^x)^2 + (r_t^y)^2 + (r_t^z)^2}$ for the length of the Bloch vector.

-
- [1] K. Brandner and U. Seifert, “Periodic thermodynamics of open quantum systems,” *Phys. Rev. E* **93**, 062134 (2016).
 [2] V. Cavina, A. Mari, and V. Giovannetti, “Slow Dynamics and Thermodynamics of Open Quantum Systems,” *Phys.*

Rev. Lett. **119**, 050601 (2017).

- [3] P. Weinberg, M. Bukov, L. D’Alessio, A. Polkovnikov, S. Vajna, and M. Kolodrubetz, “Adiabatic perturbation theory and geometry of periodically-driven systems,” *Phys. Rep.* **688**, 1 (2017).